

Silicon photonic bandpass filter based on apodized subwavelength grating with high suppression ratio and short coupling length

BOYU LIU, YONG ZHANG,* YU HE, XINHONG JIANG, JIZONG PENG, CIYUAN QIU, AND YIKAI SU

State Key Lab of Advanced Optical Communication Systems and Networks, Department of Electronic Engineering, Shanghai Jiao Tong University, Shanghai 200240, China

*yongzhang@sjtu.edu.cn

Abstract: A compact silicon bandpass filter with high sidelobe suppression is proposed and experimentally demonstrated using an apodized subwavelength grating (SWG) coupler. The device is implemented by placing a SWG waveguide next to a strip waveguide, and apodization is employed with a Gaussian profile to taper the gap between the two waveguides. A high sidelobe suppression ratio of 27 dB can be obtained with a 3-dB bandwidth of 8.8 nm and an insertion loss of 2.5 dB. Owing to the large optical phase mismatch between the two waveguides and the presence of the SWG waveguide, the coupling length of the device is reduced to 100.3 μm . The experimental results validate our proposed apodized-SWG-based contradirectional coupler (contra-DC) as a promising device in suppressing out-of-band components in coarse wavelength division multiplexed (CWDM) optical communication systems.

© 2017 Optical Society of America

OCIS codes: (130.3120) Integrated optics devices; (130.7408) Wavelength filtering devices; (050.2770) Gratings; (050.6624) Subwavelength structures; (220.1230) Apodization.

References and links

1. K. Iwatsuki, J. Kani, H. Suzuki, and M. Fujiwara, "Access and metro networks based on WDM technologies," *J. Lightwave Technol.* **22**(11), 2623–2630 (2004).
2. I. Giuntoni, P. Balladares, R. Steingrüber, J. Bruns, and K. Petermann, "WDM multi-channel filter based on sampled gratings in silicon-on-insulator," in *Optical Fiber Communication Conference* (Optical Society of America, 2011), paper OThV3.
3. X. Jiang, J. Wu, Y. Yang, T. Pan, J. Mao, B. Liu, R. Liu, Y. Zhang, C. Qiu, C. Tremblay, and Y. Su, "Wavelength and bandwidth-tunable silicon comb filter based on Sagnac loop mirrors with Mach-Zehnder interferometer couplers," *Opt. Express* **24**(3), 2183–2188 (2016).
4. W. Shi, H. Yun, C. Lin, X. Wang, J. Flueckiger, N. Jaeger, and L. Chrostowski, "Silicon CWDM Demultiplexers Using Contra-Directional Couplers," in *Conference on Lasers and Electro-Optics* (Optical Society of America, 2013), paper CTu3F.5.
5. M. T. Boroojerdi, M. Ménard, and A. G. Kirk, "Wavelength tunable integrated add-drop filter with 10.6 nm bandwidth adjustability," *Opt. Express* **24**(19), 22043–22050 (2016).
6. R. Soref, "The past, present, and future of silicon photonics," *IEEE J. Sel. Top. Quantum Electron.* **12**(6), 1678–1687 (2006).
7. B. Jalali and S. Fathpour, "Silicon photonics," *J. Lightwave Technol.* **24**(12), 4600–4615 (2006).
8. W. Shi, X. Wang, C. Lin, H. Yun, Y. Liu, T. Baehr-Jones, M. Hochberg, N. A. Jaeger, and L. Chrostowski, "Silicon photonic grating-assisted, contra-directional couplers," *Opt. Express* **21**(3), 3633–3650 (2013).
9. W. Shi, X. Wang, W. Zhang, L. Chrostowski, and N. A. Jaeger, "Contra-directional couplers in silicon-on-insulator rib waveguides," *Opt. Lett.* **36**(20), 3999–4001 (2011).
10. H. Qiu, G. Jiang, T. Hu, H. Shao, P. Yu, J. Yang, and X. Jiang, "FSR-free add-drop filter based on silicon grating-assisted contradirectional couplers," *Opt. Lett.* **38**(1), 1–3 (2013).
11. B. Naghdi and L. R. Chen, "Silicon photonic contradirectional couplers using subwavelength grating waveguides," *Opt. Express* **24**(20), 23429–23438 (2016).
12. A. V. Velasco, P. J. Bock, P. Cheben, M. L. Calvo, J. H. Schmid, J. Lapointe, D. X. Xu, S. Janz, and A. Delage, "Bandpass filter implemented with blazed waveguide sidewall gratings in silicon-on-insulator," *Electron. Lett.* **48**(12), 715–717 (2012).

13. N. Eid, R. Boeck, H. Jayatilleka, L. Chrostowski, W. Shi, and N. A. F. Jaeger, "FSR-free silicon-on-insulator microring resonator based filter with bent contra-directional couplers," *Opt. Express* **24**(25), 29009–29021 (2016).
14. A. M. Prabhu, A. Tsay, Z. Han, and V. Van, "Ultracompact SOI microring add-drop filter with wide bandwidth and wide FSR," *IEEE Photonics Technol. Lett.* **21**(10), 651–653 (2009).
15. J. Zou, X. Xia, G. Chen, T. Lang, and J.-J. He, "Birefringence compensated silicon nanowire arrayed waveguide grating for CWDM optical interconnects," *Opt. Lett.* **39**(7), 1834–1837 (2014).
16. Y. Ding, M. Pu, L. Liu, J. Xu, C. Peucheret, X. Zhang, D. Huang, and H. Ou, "Bandwidth and wavelength-tunable optical bandpass filter based on silicon microring-MZI structure," *Opt. Express* **19**(7), 6462–6470 (2011).
17. W. Shi, V. Veerasubramanian, D. Patel, and D. V. Plant, "Tunable nanophotonic delay lines using linearly chirped contradirectional couplers with uniform Bragg gratings," *Opt. Lett.* **39**(3), 701–703 (2014).
18. W. Shi, H. Yun, C. Lin, M. Greenberg, X. Wang, Y. Wang, S. T. Fard, J. Flueckiger, N. A. Jaeger, and L. Chrostowski, "Ultra-compact, flat-top demultiplexer using anti-reflection contra-directional couplers for CWDM networks on silicon," *Opt. Express* **21**(6), 6733–6738 (2013).
19. J. Wang, I. Glesk, and L. R. Chen, "Subwavelength grating filtering devices," *Opt. Express* **22**(13), 15335–15345 (2014).
20. P. J. Bock, P. Cheben, J. H. Schmid, J. Lapointe, A. Del age, S. Janz, G. C. Aers, D.-X. Xu, A. Densmore, and T. J. Hall, "Subwavelength grating periodic structures in silicon-on-insulator: a new type of microphotonic waveguide," *Opt. Express* **18**(19), 20251–20262 (2010).
21. W. Shi, H. Yun, C. Lin, J. Flueckiger, N. A. Jaeger, and L. Chrostowski, "Coupler-apodized Bragg-grating add-drop filter," *Opt. Lett.* **38**(16), 3068–3070 (2013).
22. A. D. Simard, N. Belhadj, Y. Painchaud, and S. LaRochelle, "Apodized silicon-on-insulator Bragg gratings," *IEEE Photonics Technol. Lett.* **24**(12), 1033–1035 (2012).
23. D. W. Wiesmann, C. David, R. Germann, D. Emi, and G.-L. Bona, "Apodized surface-corrugated gratings with varying duty cycle," *IEEE Photonics Technol. Lett.* **12**(6), 639–641 (2000).
24. T. Erdogan, "Fiber grating spectra," *J. Lightwave Technol.* **15**(8), 1277–1294 (1997).
25. A. Othonos and K. Kalli, *Fiber Bragg Gratings: Fundamentals and Applications in Telecommunications and Sensing* (Artech House, 1999).
26. C. Greiner, T. W. Mossberg, and D. Iazikov, "Bandpass engineering of lithographically scribed channel-waveguide Bragg gratings," *Opt. Lett.* **29**(8), 806–808 (2004).
27. A. D. Simard, M. J. Strain, L. Meriggi, M. Sorel, and S. LaRochelle, "Bandpass integrated Bragg gratings in silicon-on-insulator with well-controlled amplitude and phase responses," *Opt. Lett.* **40**(5), 736–739 (2015).
28. J. St-Yves, S. LaRochelle, and W. Shi, "O-Band Silicon Photonic Bragg-Grating Multiplexers Using UV Lithography," in *Optical Fiber Communication Conference* (Optical Society of America, 2016), paper Tu2F.7.
29. Y. Ding, H. Ou, and C. Peucheret, "Ultrahigh-efficiency apodized grating coupler using fully etched photonic crystals," *Opt. Lett.* **38**(15), 2732–2734 (2013).
30. M. Caverley, R. Boeck, L. Chrostowski, and N. A. Jaeger, "High-speed data transmission through Silicon contra-directional grating coupler optical add-drop multiplexers," in *Conference on Lasers and Electro-Optics* (Optical Society of America, 2015), paper JTh2A.41.
31. B. Liu, Y. Zhang, X. Jiang, Y. He, C. Qiu, and Y. Su, "High-suppression-ratio silicon bandpass filter using apodized subwavelength grating coupler," in *CLEO-PR, OECC and PGC Conference* (Optical Society of America, 2017), paper s1944.

1. Introduction

Ever-increasing network capacity for broadband access is driving the demand for high-performance filtering technologies in coarse wavelength division multiplexed (CWDM) optical communication networks [1–5]. Due to the advantages of compact device footprint, low cost, low power consumption, and high robustness, integrated optical add-drop filters based on silicon photonics are expected to be the key components for next-generation CWDM networks [6–8]. Many schemes were proposed to realize silicon bandpass filtering devices, including Bragg gratings [8–12], microring resonators (MRRs) [13, 14], arrayed waveguide grating [15], Mach–Zehnder interferometer (MZI) [16] and so on. Filters based on Bragg gratings take advantage of free spectral range (FSR) free operation. However, a two-port Bragg grating operates in reflection mode, which requires an optical isolator [8]. Grating-assisted contra-directional couplers (contra-DCs) exhibit the merits of single passband operation and great design flexibility, which are promising for add-drop operations in CWDM systems [17, 18].

Among the grating-assisted contra-DCs, the contra-DC using subwavelength grating (SWG) is attractive since it offers the benefits including short coupling length, high fabrication tolerance, and no significant ripples in the passband [11, 19, 20]. However, the

main challenge for the SWG-based contra-DC lies in its strong sidelobes, which results in high crosstalk between neighboring channels in CWDM (de)multiplexers. Apodization is a widely used technique in tailoring the spectra of gratings and suppressing sidelobes [21–30]. Recently, an apodized Bragg grating-assisted contra-DC was proposed to realize a high sidelobe suppression ratio of 30 dB with a coupling length of 829.4 μm [21].

In this paper, we experimentally demonstrate a silicon contra-DC using an apodized SWG waveguide to realize a high sidelobe suppression ratio of 27 dB with a short coupling length of 100.3 μm . The proposed structure consists of two asymmetric waveguides where a SWG waveguide is placed next to a strip waveguide. Due to the large phase mismatch between the two waveguides and the presence of the SWG waveguide, the coupling length can be reduced to 100.3 μm , which is much shorter than that of the apodized Bragg grating-assisted contra-DCs [21]. Moreover, the high sidelobes can be effectively suppressed through apodization by tapering the coupling strength in the contra-DC with a Gaussian profile of the gap between the strip waveguide and the SWG waveguide. In the experiment, a high sidelobe suppression ratio of 27 dB at the drop port is achieved with an optimized design by varying the apodization index and the gap distance, which is much improved compared to our previous result of 20 dB [31].

2. Device structure and operation principle

Figures 1(a) and (b) depict the 3D and top views of the proposed silicon contra-DC based on an apodized SWG, respectively. The coupler-apodized contra-DC is composed of two waveguides, the upper waveguide is a straight waveguide and the bottom waveguide is a curved SWG waveguide. SWG tapers at the two ends of the apodized SWG waveguide are used for the mode transition between the SWG waveguide and the straight waveguides. In the coupling region, the effective contradirectional coupling can be realized over a short coupling length since undesired codirectional coupling is suppressed due to the phase mismatch between the two asymmetric waveguides, while the contradirectional coupling is enhanced by the relatively large coupling coefficient owing to the grating mechanism [11]. Meanwhile, the sidelobes can be effectively suppressed by tapering the coupling strength, i.e., the coupling strength at the center of the coupling region is the strongest, while the coupling strength gradually reduces away from the center of the coupling region. The coupling gap $G(n)$ is

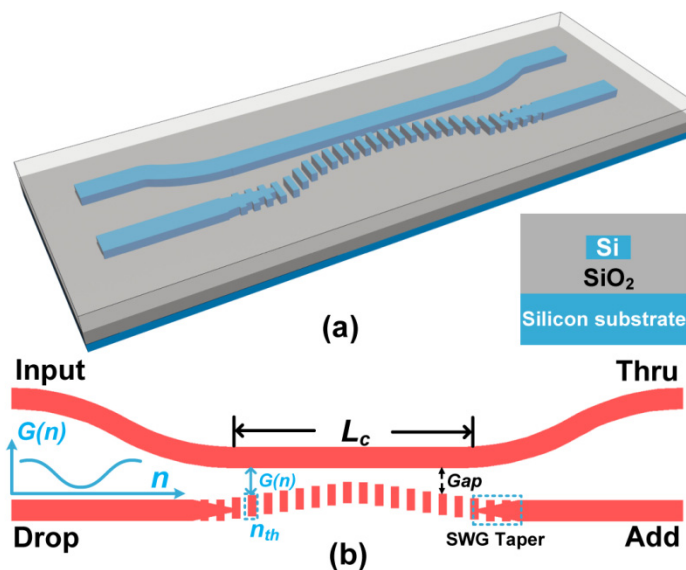


Fig. 1. Schematic configuration of the proposed silicon apodized-SWG-based contra-DC, (a) the 3D view, (b) the top view. $G(n)$: the coupling gap of the n -th period of the grating.

designed as a Gaussian function of n -th period of the grating, which is given by [8, 21]:

$$G(n) = G_{\min} + R \left[1 - e^{-\frac{a(n-0.5N)^2}{N^2}} \right]. \quad (1)$$

where G_{\min} is the minimum gap at the center of the coupling area, which is chosen to be 200 nm in the uniform design. The constant R is chosen to be 1 μm . The apodization index a determines the curvature of the SWG waveguide, which relates to the coupling strength of the two waveguides. A trade-off between the sidelobe suppression ratio and the insertion loss is required. A larger a can lead to a higher suppression ratio, however, it results in a larger insertion loss. The period number N is chosen as 300. The period and the duty cycle of the SWG are $\Lambda = 378$ nm and $\eta = 50\%$, respectively. Thus the coupling length is 100.3 μm , and the 3-dB bandwidth of the device is ~ 10 nm from the simulation, which is compatible with the existing CWDM networks [4].

3. Simulation results

Three-dimensional finite-difference time-domain (3D-FDTD) method is applied to simulate the proposed apodized-SWG-based structure. Figure 2(a) shows the simulated spectra at the through and drop ports of contra-DCs by using the uniform grating and the apodized grating ($a = 5$), respectively. The simulation parameters are $L_c = 100.3$ μm , $\Lambda = 378$ nm and $\eta = 50\%$. The widths of the upper strip waveguide and the bottom SWG waveguide are both 500 nm. In the simulations, the uniform SWG-based device with a constant 200-nm gap has strong sidelobes, which are as high as -5.1 dB at an off-center wavelength of 6.8 nm, and are as high as -8.3 dB with a 12-nm detuning. The blue solid curve shows that the sidelobes of the contra-DC are effectively suppressed with the apodized SWG at an apodization index $a = 5$, $G_{\min} = 200$ nm. The suppression ratio of the highest sidelobe has been improved by ~ 23.4 dB, and the rest sidelobes are below -45 dB.

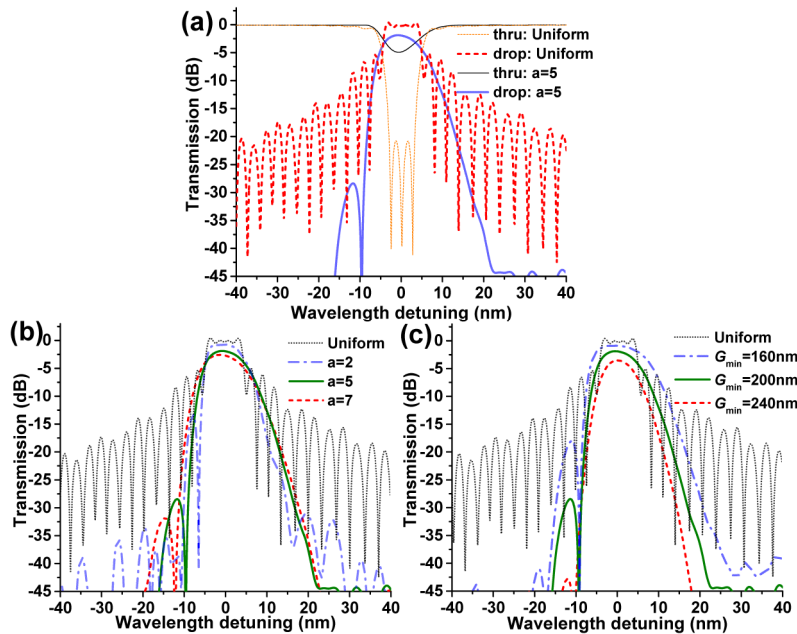


Fig. 2. (a) Simulated transmission spectra of through and drop ports of contra-DCs with a uniform grating and one with an apodized grating, showing the sidelobe suppression in the apodized design. (b), (c) Calculated drop-port spectra of the contra-DCs with (b) varied apodization index a while $L_c = 100.3$ μm , $G_{\min} = 200$ nm and (c) varied G_{\min} with $L_c = 100.3$ μm , $a = 5$, respectively.

To obtain a better sidelobe suppression of the contra-DC using the apodized SWG, both the apodization index a and the minimum gap distance G_{\min} are investigated and optimized. Figure 2(b) illustrates the simulated transmission spectral evolution of the drop-port for a contra-DC at different apodization indices a . As a increases, the coupling strength decreases faster away from the center of the coupling region, thus leading to the higher sidelobe suppression ratio. It can be seen that when the apodization index a increases from 5 to 7, the suppression ratio is improved by ~ 4 dB at the expense of the insertion loss increasing from ~ 1.8 dB to ~ 2.6 dB. The excess insertion loss is attributed to the lower average coupling coefficient caused by the curvature of the apodized SWG with the same coupling length. Simulation results show that the reflection responses of the uniform and the apodized SWGs are lower than -18 dB and -27 dB, respectively.

Compared to the uniform design, the bandwidth of the apodized design is slightly expanded which can be optimized by adjusting G_{\min} as depicted in Fig. 2(c). It shows a larger gap distance G_{\min} leads to a narrower drop-port bandwidth and lower sidelobes, but a larger insertion loss. Therefore, to realize a desired spectrum of the passband, both the apodization index a and the gap distance G_{\min} should be carefully optimized.

4. Device fabrication and measured transmission spectra

In the experiment, multiple apodized-SWG-based contra-DCs were fabricated on a silicon-on-insulator (SOI) wafer with a 220-nm-thick top silicon layer and a 3- μm -thick buried dioxide layer. E-beam lithography (EBL, Vistec EBPG 5200) was used to define the device structures on the ZEP520A resist. Then the patterns were transferred to the top silicon layer by an inductively coupled plasma (ICP) etching process. A 1- μm -thick silica layer was deposited over the whole device as the upper cladding by plasma-enhanced chemical vapor deposition (PECVD). The transmission spectra of the fabricated devices are measured by using a tunable continuous wave (CW) laser (Keysight 81960A) scanning from 1530 nm to 1620 nm with a step size of 5 nm. The output spectra are obtained by recording the output optical power. Both the widths of the strip and the apodized SWG waveguides are 500 nm. The period and the duty cycle of the apodized SWG are 378 nm and 50%, respectively. The device footprint is $\sim 113 \times 2 \mu\text{m}^2$. The scanning electron microscope (SEM) photo of a fabricated contra-DC using the apodized SWG is shown in Fig. 3(a). Figure 3(b) depicts a zoom-in SEM graph of the coupling region of the contra-DC. The magnified micrograph of the strip and the SWG waveguides is presented in Fig. 3(c).

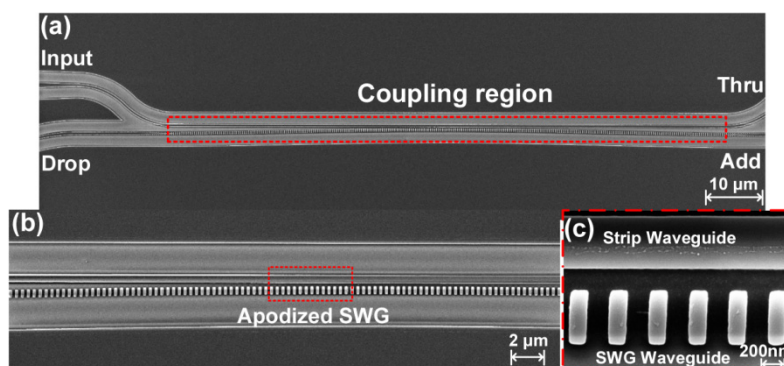


Fig. 3. (a) Scanning electron microscope (SEM) photo of a fabricated contra-DC based on apodized SWG. (b) Zoom-in SEM graph of the coupling region. (c) Magnified micrograph of the strip and SWG waveguide.

Figure 4 shows the measured responses at the drop ports of the fabricated apodized-SWG-based contra-DCs. The responses are normalized to the transmission spectrum of a strip waveguide with grating couplers. When $a = 0$, the spectrum at the drop port of the contra-DC

using the uniform SWG with a constant 200-nm gap distance shows strong presence of sidelobes. The sidelobes at a 10-nm detuning are ~ 4.5 dB, and are still as high as -7.5 dB at a 22-nm off-center wavelength. In our experiment, the apodization index a is chosen as 5, which is a trade-off between the insertion loss and the sidelobe suppression ratio. It can be seen that the apodized-SWG-based devices show much improved sidelobe suppression ratios.

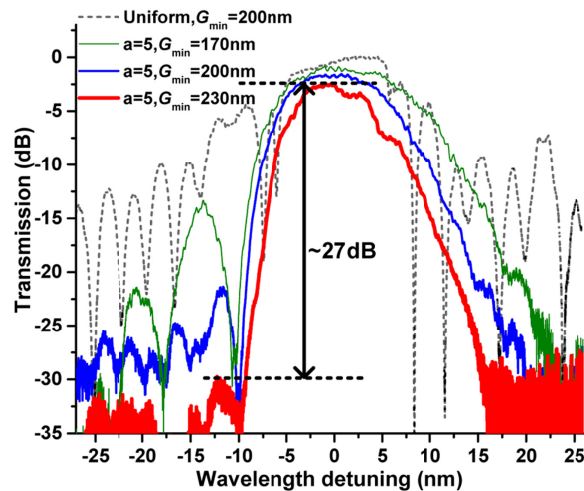


Fig. 4. Measured drop-port spectra of the contra-DCs with different G_{\min} values.

Furthermore, to achieve a high sidelobe suppression ratio of the contra-DCs at $a = 5$, devices with different minimum gap distances of G_{\min} were fabricated and then measured as shown in Fig. 4. The red solid curve shows that with an optimized value of $G_{\min} = 230$ nm, a high sidelobe suppression ratio of 27 dB at the 12-nm off-center wavelength detuning has been obtained. Other sidelobes are all suppressed below -30 dB. Note that the noise at the longer wavelength is mainly attributed to the passband edges of the grating couplers that result in large fluctuation in the normalization process. In comparison with the coupler having the uniform SWG, the 3-dB bandwidths of the contra-DCs are slightly expanded. A larger gap distance leads to a narrower drop-channel bandwidth and lower sidelobes.

5. Summary

We have experimentally demonstrated a silicon SWG-based contra-DC with high sidelobe suppression by tailoring the coupling strength between the strip waveguide and the SWG waveguide. A short coupling length of $100.3 \mu\text{m}$ is obtained, and a high sidelobe suppression ratio of 27 dB is experimentally demonstrated. These make the proposed silicon apodized-SWG-based contra-DC promising for CWDM optical communication systems.

Funding

National Natural Science Foundation of China (NSFC) (61605112, 61235007, 61505104), 863 High-Tech Program (2015AA017001); Science and Technology Commission of Shanghai Municipality (15ZR1422800, 16XD1401400).

Acknowledgments

We acknowledge the support of device fabrication by the Center for Advanced Electronic Materials and Devices of Shanghai Jiao Tong University.